# Electronic Supplementary Information

# Double-shelled Yolk-Like Structure as an Ideal Magnetic Support of Tiny Gold Nanoparticles for Nitrophenol Reduction

**Tao Zeng,[a] Xiaole Zhang,[a,b] Saihua Wang,[c] Yurong Ma,[a] Hongyun Niu,[a] and Ya-qi Cai*[a]**

[a] *State Key Laboratory of Environmental Chemistry and Ecotoxicology, Research Center for Eco-Environmental Sciences, Chinese Academy of Sciences, P.O. Box 2871, Beijing 100085, China.*
*Tel: +86-10-6284-9182; E-mail:caiyaqi@rcees.ac.cn;*
[b] *College of life science, Hebei United University, Tangshan, Hebei, 063000, China;*

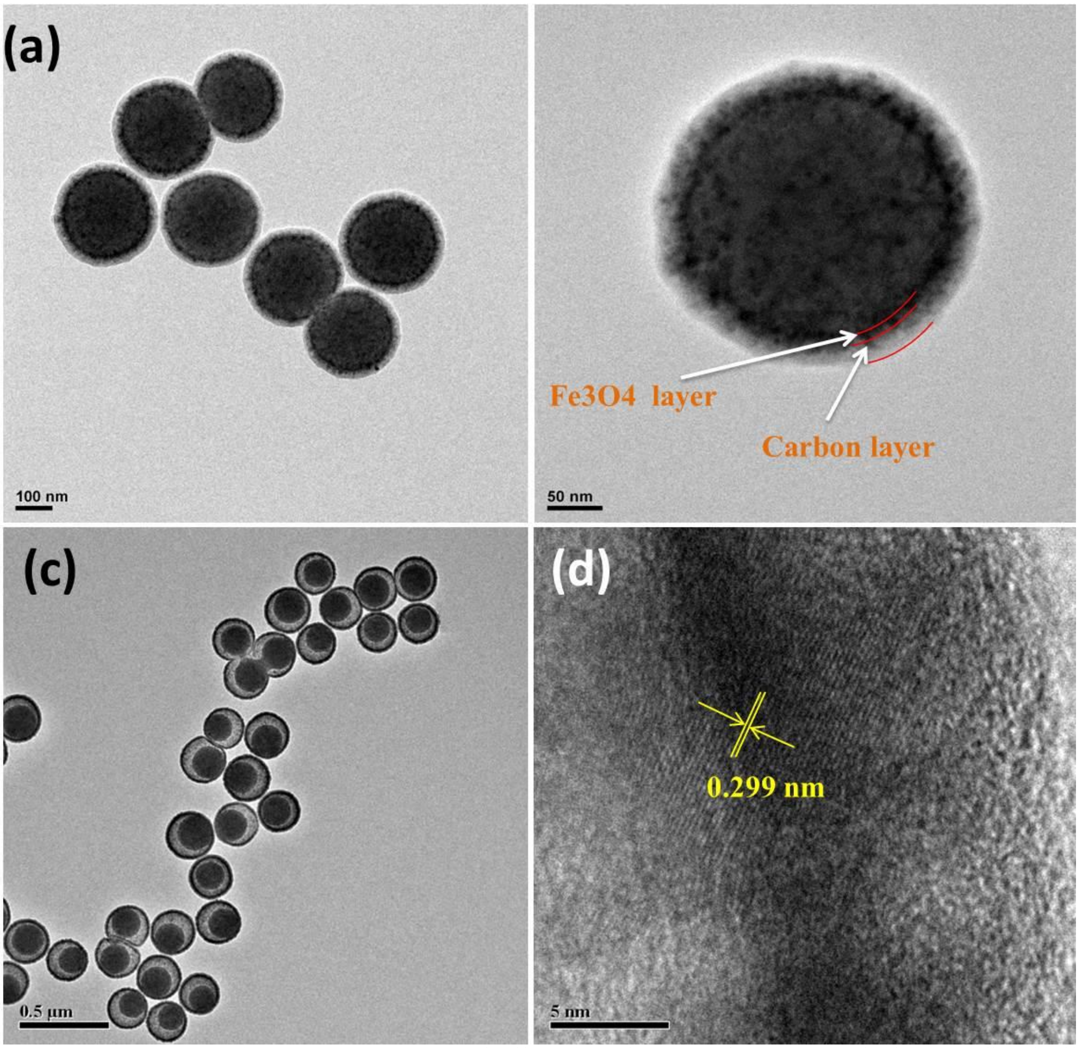

**Figure S1.** TEM images of core-shell $SiO_2@Fe_3O_4/C$ (a and b), yolk-shell $SiO_2@Fe_3O_4/C$ (c); HRTEM image of the shell (d). **Figure S1**a shows sphere-like morphology of the particles and the size is around 260 nm. From a higher magnification TEM image (Figure S1b), it can be seen that the particles exhibit a defined core-shell structure with a core of about 230 nm in diameter and a shell of 35 nm thickness. Clearly, the shell is composed of a deep-contrast inner layer and a light-contrast outer layer, which are assigned to $Fe_3O_4$ and carbon component, respectively. Apart from the common functions (protecting the core, allowing the species diffusion), this double-layered shell can endow the materials with some new merits such as the superparamagnetism and the large loading capacity of guest NPs. A high-resolution transmission electron microscopy (HRTEM) image of the shell (Figure S1d) displays regular lattice fringes with an inter-planar spacing of 0.299 nm, which is highly consistent with the *d* value of the (220) planes of the magnetite structure.[1]

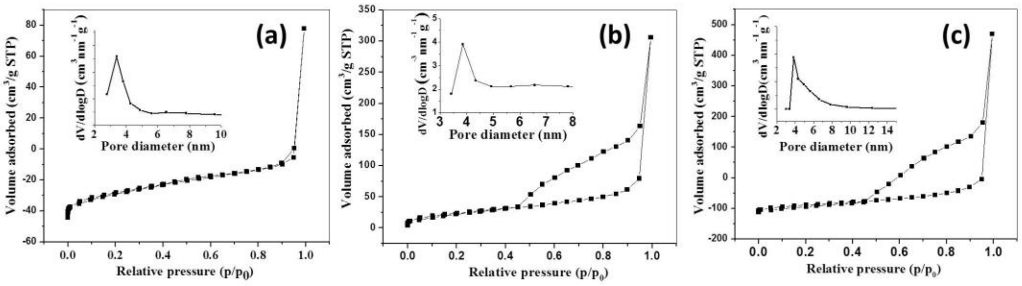

**Figure S2.** $N_2$ adsorption-desorption isotherms of core-shell $SiO_2@Fe_3O_4/C$ (a), yolk-shell $SiO_2@Fe_3O_4/C$ (b), and hollow $Fe_3O_4/C$ (c). All the adsorption-desorption isotherms show a type IV behavior. The large hysteresis loops appearing in the latter two curves confirm the cage-like mesoporous structure (Figure 3b and c), which contains large cages as well as small mesopores in the framework.[2] These are in good agreement with the yolk-shell and hollow nanostructures observed in TEM images.

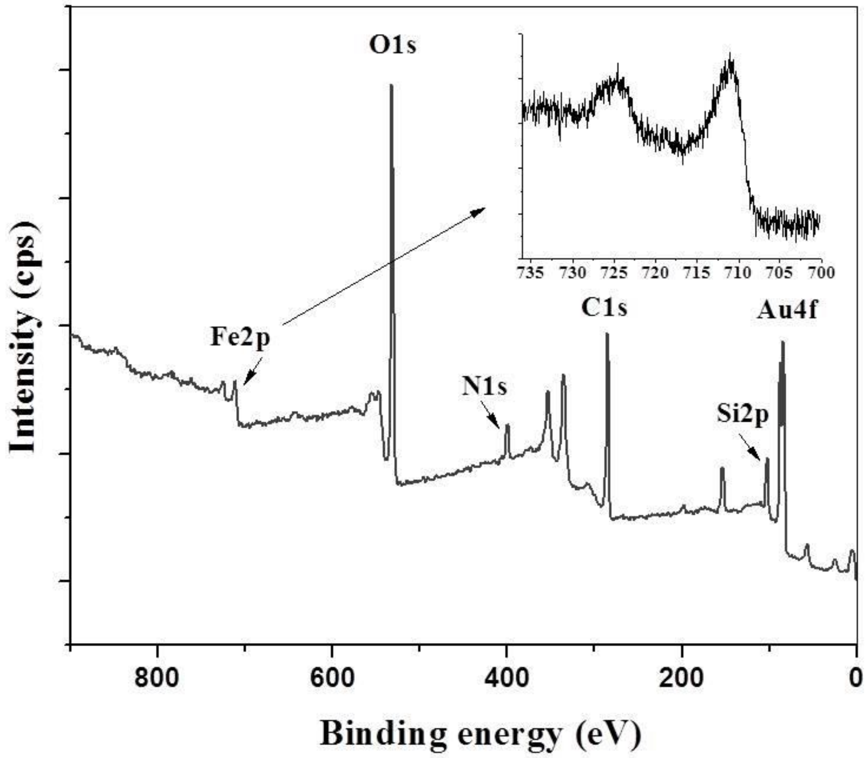

**Figure S3.** Wide scan survey XPS spectrum of yolk-shell $SiO_2@Fe_3O_4/C@Au$ composites.

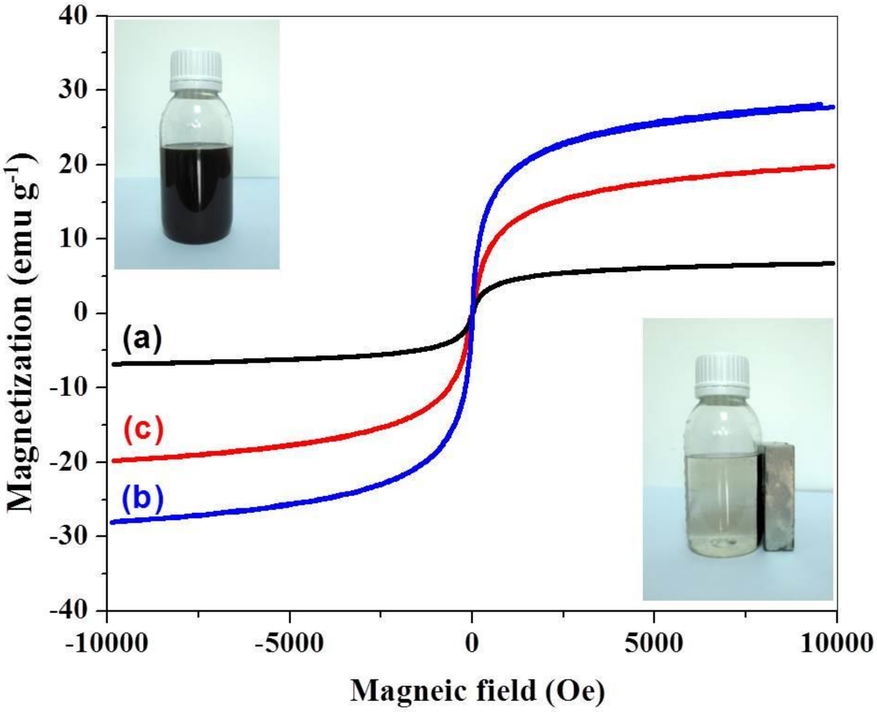

**Figure S4.** VSM curves of core-shell $SiO_2@Fe_3O_4/C$ (a), yolk-shell $SiO_2@Fe_3O_4/C$ (b), and yolk-shell $SiO_2@Fe_3O_4/C@Au$ (c). The insets show the digital images of materials before (left) and after (right) isolation by an external magnetic field. No obvious remanence or coercivity is found in all the three magnetization curves, suggesting the superparamagnetic character of each composite. This superparamagnetism contributes to avoiding the aggregation of the nanocomposites caused by the residual magnetism after removal of the applied magnetic field.

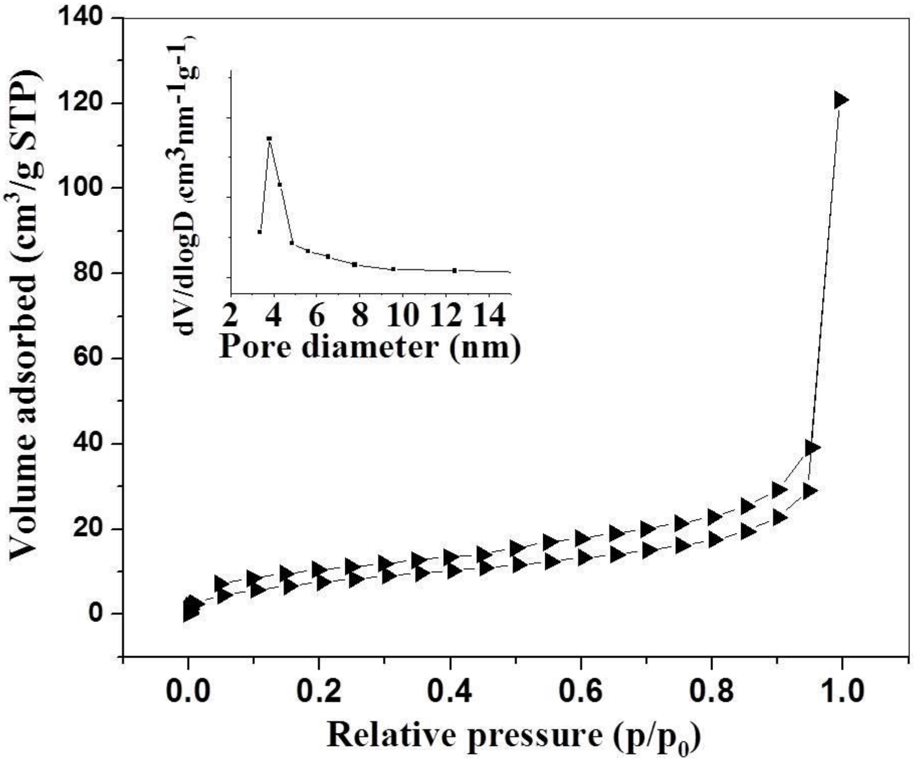

**Figure S5.** $N_2$ adsorption-desorption isotherms of yolk-shell $SiO_2@Fe_3O_4/C@Au$ composites.

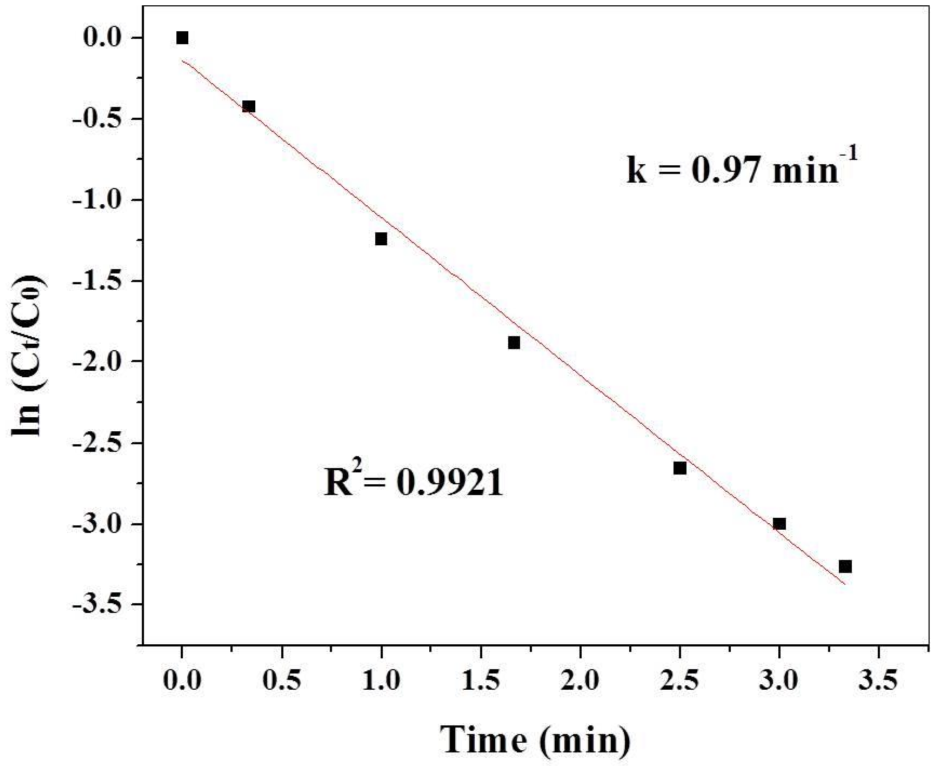

**Figure S6.** Plot of ln ($C_t/C_0$) *versus* reaction time. $C_t$ and $C_0$ are the concentrations of 4-nitrophenol at time *t* and at the beginning, respectively.

**Table S1.** Comparison of catalytic activity for 4-nitrophenol reduction by Au based nanocatalysts

| Catalyst | Moles of 4-nitrophenol | Amount of catalyst | Required time | Au content | TOF[a] | Reference |
|---|---|---|---|---|---|---|
| $Fe_3O_4$@PDA-Au | 0.85 umol | 0.05 mg | 19 min | $1.09\times10^{-2}$ umol | 4.1 $min^{-1}$ | [3] |
| Yolk-shell Au@[Na]-HAMS | 30 umol | 10 mg | 12 min | - | - | [4] |
| Dumbbell-like $Fe_3O_4$-Au | 0.4 umol | 2 mg | 10 min | 1.9 umol | 0.02 $min^{-1}$ | [5] |
| $Fe_3O_4$@$SiO_2$-Au@m$SiO_2$ | 0.5 umol | 3 mg | 15 min | $3.35\times10^{-1}$ umol | 0.1 $min^{-1}$ | [6] |
| $Fe_3O_4$@$SiO_2$-LBL-Au | 0.5 umol | 0.03 mg | 15 min | $2.48\times10^{-3}$ umol | 13.4 $min^{-1}$ | [7] |
| Au-EGCG-CF | 1 umol | - | 30 min | 1 umol | 0.033 $min^{-1}$ | [8] |
| Au/PMMA | 1.35 umol | 3.5 mg | 10 min | $8.8\times10^{-2}$ umol | 1.53 $min^{-1}$ | [9] |
| Poly(DVB-co-AA)@Au | 39.1 umol | 6 mg | 72 min | $1.47\times10^{-1}$ umol | 3.7 $min^{-1}$ | [10] |
| Rattle-type $SiO_2$@Au/PEGDMA | 0.1 umol | 0.01 mg | 50 min | $0.92\times10^{-3}$ umol | 2.2 $min^{-1}$ | [11] |
| Yolk-double shell $SiO_2$@$Fe_3O_4$-C@Au | 0.5 umol | 0.05 mg | 3.3 min | $8.63\times10^{-3}$ umol | 17.4 $min^{-1}$ | **This work** |

[a] Calculated by the moles of 4-NP reduced per mole of Au content per consumed time.

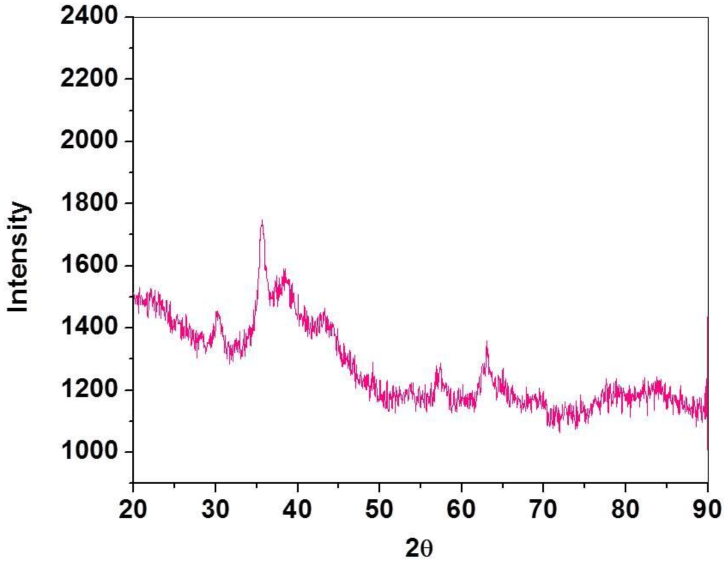

**Figure S7.** XRD pattern of yolk-shell $SiO_2$@$Fe_3O_4$/C@Au after used. The spectrum is similar to that of catalyst before used and the size of Au NPs calculated by Scherrer formula almost remain unchanged (3.1 nm), further suggesting the stability of the catalyst.

---

## Reference:

[1] S. H. Liu, F. Lu, R. M. Xing, J. J. Zhu, Chem. Eur. J. 2011, 17, 620.

[2] a) J. C. Park, J. U. Bang, J. Lee, C. H. Ko, H. Song, J. Mater. Chem. 2010, 20, 1239; b) J. C. Park, H. J. Lee, H. S. Jung, M. Kim, H. J. Kim, K. H. Park, H. Song, Chemcatchem 2011, 3, 755.

[3] T. Zeng, X. L. Zhang, H. Y. Niu, Y. R. Ma, W. H. Li, Y. Q. Cai, *Appl. Catal. B: Environ.* 2013, *134-135*, 26.

[4] X. Fang, Z. Liu, M.-F. Hsieh, M. Chen, P. Liu, C. Chen, N. Zheng, ACS Nano 2012, *6*, 4434.

[5] F. H. Lin, R. A. Doong, *J. Phys. Chem. C* 2011, *115*, 6591.

[6] Y. H. Deng, Y. Cai, Z. K. Sun, J. Liu, C. Liu, J. Wei, W. Li, C. Liu, Y. Wang, D. Y. Zhao, *J. Am. Chem. Soc.* 2010, *132*, 8466.

[7] Y. H. Zhu, J. H. Shen, K. F. Zhou, C. Chen, X. L. Yang, C. Z. Li, *J. Phys. Chem. C* 2011, *115*, 1614.

[8] H. Wu, X. Huang, M. M. Gao, X. P. Liao, B. Shi, *Green Chem.*, 2011, *13*, 651.

[9] Kuroda, K., T. Ishida, and M. Haruta, *J. Mol. Catal. A-chem.*, 2009, *298*, 7.

[10] Liu, W., X.L. Yang, and W.Q. Huang, *J. Colloid Interf. Sci.*, 2006, *304*, 160.

[11] B. Liu, W. Zhang, H. Feng, X. Yang, *Chem Commun (Camb)* **2011**, *47*, 11727.